DTU Library

Self-consistent linear-muffin-tin-orbitals coherent-potential technique for bulk and surface calculations: Cu-Ni, Ag-Pd, and Au-Pt random alloys

Abrikosov, I. A.; Skriver, Hans Lomholt

Self-consistent linear-muffin-tin-orbitals coherent-potential technique for bulk and surface calculations: Cu-Ni, Ag-Pd, and Au-Pt random alloys

I. A. Abrikosov

*Chair for Theoretical Physics, Moscow Institute for Steel and Alloys, Moscow, Russia
and Physics Department, Technical University of Denmark, DK-2800 Lyngby, Denmark*

H. L. Skriver

Physics Department, Technical University of Denmark, DK-2800 Lyngby, Denmark

We present an efficient technique for calculating surface properties of random alloys based on the coherent-potential approximation within a tight-binding linear-muffin-tin-orbitals basis. The technique has been applied in the calculation of bulk thermodynamic properties as well as (001) surface energies and work functions for three fcc-based alloys (Cu-Ni, Ag-Pd, and Au-Pt) over the complete concentration range. The calculated mixing enthalpies for the Ag-Pd and Au-Pt systems agrees with experimental values, and the calculated concentration dependence of the lattice parameters agrees with experiment for all three systems. We find that the calculated surface energies and work functions in the unsegregated case exhibit a small positive deviation from a linear concentration dependence. Finally, we performed a segregation analysis based on the calculated surface energies by means of a simple thermodynamic model and found in complete agreement with experiment that the noble metals segregate strongly towards the surface of their alloys.

I. INTRODUCTION

The properties of solid surfaces are of considerable scientific interest because they play an important role in such phenomena as catalysis, chemisorbtion, and corrosion. Recently there has been significant progress in *ab initio* calculations of the electronic structure of surfaces of ordered materials using a Green's-function technique.[1–5] It appears that one may calculate surface-related properties such as surface tension and work function with a high degree of accuracy. In this context, random metallic alloys represent a large class of technologically important materials, the surface properties of which have only been investigated in a few cases.

One of the most common approximations for treating disordered alloys is the coherent-potential approximation (CPA),[6,7] which is based on the assumption that the initial alloy may be replaced by an ordered effective medium, the parameters of which must be determined self-consistently. This approximation is extensively used in bulk electronic-structure calculations for random alloys, although such calculations are rather time consuming. When a two-dimensional defect such as a surface or an interface is introduced, the effective medium loses some of its translation invariance and the numerical problems increase considerably. Hence there are at present only a limited number of surface calculations for disordered materials based on the CPA.[8–10]

Here we present an efficient technique for calculating surface properties of random alloys based on the coherent-potential approximation in a tight-binding linear-muffin-tin-orbitals (LMTO) basis within the atomic sphere approximation (ASA). It allows us to solve the electronic-structure problem for bulk as well as for the surface from first principles within a single scheme. Furthermore, the one-electron equations are solved self-consistently, and hence it is possible to determine a number of important thermodynamic properties for the systems under consideration.

We apply our technique to three fcc-based random alloys Cu-Ni, Ag-Pd, and Au-Pt, which have been considered as heterogeneous catalysist. Previously, Kudrnovsky *et al.* considered the electronic structure of the (100) surface of random Ag-Pd alloys[8] and presented a self-consistent calculation of a random Ag-Pd overlayer on a Ag (100) substrate.[9] Here we present *ab initio* calculations of lattice parameters, mixing enthalpies, surface energies, and work functions for three alloy systems over the complete concentration range and we use the surface energies calculated for the unsegregated surfaces in conjunction with a simple thermodynamic model to perform segregation analyses for the (100) surface of Cu-Ni, Ag-Pd, and Au-Pt alloys.

II. LMTO-CPA METHOD FOR BULK

A. KKR-ASA Green's function

The one-electron Green's function may be regarded as the key quantity in the calculation of electronic and thermodynamic properties of solids. Within the ASA it is most conveniently represented by the Green's-function matrix g defined by the KKR-ASA equation[11]

$$[\mathbf{P}^\alpha(z) - \mathbf{S}^\alpha(\mathbf{k})]\mathbf{g}^\alpha(\mathbf{k}, z) = 1. \qquad (1)$$

Here z is a complex energy, $\mathbf{P}$ and $\mathbf{S}$ are LMTO potential functions and structure constants matrices, respectively, and the superscript α denotes the LMTO representation to be used. The structure constants matrix $\mathbf{S}^\alpha$ is connected to the conventional LMTO structure constants matrix $\mathbf{S}^0$ by the Dyson equation[12]

$$S^\alpha_{R'L',RL} = S^0_{R'L',RL} + \sum_{R''L''} S^0_{R'L',R''L''}\alpha_{l''} S^\alpha_{R''L'',RL},$$

(2)

where R denotes lattice sites, L is the combined angular-momentum quantum numbers (l,m), and α is a diagonal screening matrix. The potential function may be parameterized in the form[12]

$$P^{\alpha j}_{Rl}(z) = \frac{C^j_{Rl} - z}{(C^j_{Rl} - z)(\gamma^j_{Rl} - \alpha_l) + \Delta^j_{Rl}}$$

(3)

by means of the center C, bandwidth Δ, and γ potential parameters obtained from the solution of the radial Schrödinger equation for an element j at an arbitrary energy E_ν in the energy range of interest.

B. LMTO-CPA formalism

The basic idea behind the CPA is the replacement of the initial random alloy by an ordered lattice of effective scatterers. In the single-site approximation the properties of these effective atoms have to be determined self-consistently by the condition that the scattering of electrons off real atoms embedded in the effective medium vanish on the average. For a disordered binary alloy A_cB_{1-c} this condition may be written as

$$\tilde{g}^\alpha_{RL,RL'}(z) = (V_{\text{BZ}})^{-1}\int_{\text{BZ}} d\mathbf{k}\{[\tilde{\mathbf{P}}^\alpha(z) - \mathbf{S}^\alpha(\mathbf{k})]^{-1}\}_{RL,RL'},$$

(4)

$$\tilde{P}^\alpha_R(z) = cP^{\alpha A}_R(z) + (1-c)P^{\alpha B}_R(z)$$
$$+[P^{\alpha A}_R(z) - \tilde{P}^\alpha_R(z)]\tilde{g}^\alpha_{RR}(z)[P^{\alpha B}_R(z) - \tilde{P}^\alpha_R(z)],$$

(5)

in the single-site approximation and within a tight-binding LMTO basis.[13] In (4) and (5) the tilde refers to the effective scatterer and V_{BZ} is the volume of the Brillouin zone.

If the two coupled CPA equations (4) and (5) are solved self-consistently, one may obtain the Green's-function matrices $\mathbf{g}^{\alpha j}$ for the alloy components $j = A, B$ as the

Green's function for a single impurity in the ideal effective lattice,[11] i.e.,

$$g^{\alpha j}_R(z) = \{[\tilde{g}^\alpha_{RR}(z)]^{-1} + P^{\alpha j}_R(z) - \tilde{P}^\alpha_R(z)\}^{-1}.$$

(6)

As a result, one may calculate the moments of the state density $m^{jq'q''}_{RL'L''}$ for the A and B atoms as the contour integral

$$m^{jq'q''}_{RL'L''} = \frac{1}{2\pi i}\oint dz(z - E_{\nu Rl'})^{q'} G^{\gamma j}_{RL',RL''}(z)(z - E_{\nu Rl''})^{q''}$$

(7)

and the valence charge density $n^{jv}_R(r)$ in the corresponding atomic spheres as the one-center expansion

$$n^{jv}_R(r) = (4\pi)^{-1}\sum_L \{\,[\phi^j_{Rl}(r)]^2 m^{j00}_{RLL}$$
$$+2[\phi^j_{Rl}(r)\dot{\phi}^j_{Rl}(r)]m^{j10}_{RLL}$$
$$+[\dot{\phi}^j_{Rl}(r)\dot{\phi}^j_{Rl}(r)$$
$$+\phi^j_{Rl}(r)\ddot{\phi}^j_{Rl}(r)]m^{j20}_{RLL}\}.$$

(8)

Here the contour must enclose the occupied valence states and ϕ, $\dot{\phi}$, and $\ddot{\phi}$ denote the partial wave and its first and second energy derivatives, respectively, evaluated at the energy $E_{\nu Rl}$. The Hamiltonian Green's function G which enter the contour intgral (7) is found by the transformation

$$G^\gamma(z) = \frac{1}{z - V^\alpha} + \frac{\sqrt{\Gamma^\alpha}}{z - V^\alpha}g^\alpha(z)\frac{\sqrt{\Gamma^\alpha}}{z - V^\alpha},$$

(9)

where the representation-dependent potential parameters V^α and Γ^α are

$$V^\alpha = C - \frac{\Delta}{\gamma - \alpha}, \qquad \Gamma^\alpha = \frac{\Delta}{(\gamma - \alpha)^2}.$$

(10)

Knowing the charge density of the alloy components one may calculate new component potential functions, repeat the CPA self-consistency loop (4) and (5), and obtain new charge densities. When eventually the CPA and the charge self-consistency loops are satisfied simultaneously, one may calculate the total energy of the random alloy $E^{\text{alloy}}_{\text{tot}}$. In the framework of the single-site CPA this may be written as[7]

$$E^{\text{alloy}}_{\text{tot}} = cE^A + (1-c)E^B + E_M,$$

(11)

where the components energies $E^{j=A,B}$ within the frozen-core and local-density approximations have the form[11]

$$E^j = \sum_R \sum_L (E^j_{\nu Rl}m^{j00}_{RLL} + m^{j10}_{RLL}) - \frac{1}{\sqrt{4\pi}}\int_R d^3r\, n^{iv}_R(r)V_R(r)$$

$$-\sum_R \frac{1}{\sqrt{4\pi}}\int_R d^3r\, n^{jv}_R(r)\frac{2Z^j_R}{r} + \sum_R \frac{1}{4\pi}\int_R d^3r\, n^{jv}_R(r)[\tfrac{1}{2}V^{jv}_{C;R}(r) + V^{jc}_{C;R}(r)]$$

$$+\sum_R \frac{1}{\sqrt{4\pi}}\int_R d^3r\, n^j_R(r)\epsilon_{\text{xc}}[n^j_R(r)] - \sum_R \frac{1}{\sqrt{4\pi}}\int_R d^3r\, n^{jc}_R(r)\epsilon_{\text{xc}}[n^{jc}_R(r)].$$

(12)

TABLE I. Valence charge in the atomic spheres of the components for bulk and for surface layer in Cu-Ni, Ag-Pd, and Au-Pt alloys.

Alloy	Element	Valence charge (electrons)	
		Surface layer	Bulk
$Cu_{50}Ni_{50}$	Cu	10.71	11.00
	Ni	9.71	10.00
$Ag_{50}Pd_{50}$	Ag	10.72	10.97
	Pd	9.78	10.03
$Au_{50}Pt_{50}$	Au	10.70	10.99
	Pt	9.71	10.01

In (12) the R summation for the bulk case runs over the site $R = 0$ only, m^{00} and m^{10} are moments of the state density, $n_R = n_R^v + n_R^c$ is the spherically symmetric charge density inside each atomic sphere at R separated into valence v and core c contributions, Z_R is the atomic number, $V_{C;R}$ is the electrostatic potential, V_R is the effective one-electron potential, and $\epsilon_{\rm xc}$ is the exchange-correlation energy density.

In most CPA calculations the Madelung energy contribution E_M to (11) is calculated from the average charge transfer $\bar{Q}$

$$\bar{Q} = cQ^A + (1 - c)Q^B, \tag{13}$$

where Q^j is the net charge in the atomic sphere. Owing to the charge neutrality condition $cQ^A = -(1 - c)Q^B$, (13) results in zero average charge transfer and hence the Madelung energy vanishes, i.e.,

$$E_M = 0. \tag{14}$$

This choice of Madelung energy based on the average charge transfer (13) is not always a good approximation[14] and instead one may calculate the average Madelung energy.[15] However, for the systems considered in the present work, the component charge transfer is practically zero (Table I) and hence (14) is a good approximation.

C. Effective procedure for the charge self-consistency

The main problem of all the CPA-based methods is the large amount of numerical calculations that has to be carried out to solve the coupled CPA equations (4) and (5). In the past one has developed effective algorithms for this purpose (see, for example, Ref. 16), but the problem reappears when charge self-consistency is included. In this case one may have to perform approximately 100 iterations each of which requires the time-consuming calculation of the integral (4).

In conventional LMTO calculations[17] the number of time-consuming band iterations is greatly reduced by the LMTO scaling principle. For surface calculations one may introduce a similar technique based on the solution of the linearized Dyson equation, which reduces the number of times the complete Dyson equation must be solved by one order of magnitude.[5] The principle is that only

when charge self-consistency has been obtained by means of an approximate state density or Green's function is the complete electronic structure recalculated.

In LMTO-CPA calculations the effective-medium Green's function at the $(i + 1)$th iteration is related to the one at the ith iteration by the Dyson equation

$$\tilde{\mathbf{g}}^{(i+1)} = \tilde{\mathbf{g}}^i - \tilde{\mathbf{g}}^i(\tilde{\mathbf{P}}^{(i+1)} - \tilde{\mathbf{P}}^i)\tilde{\mathbf{g}}^{(i+1)}, \tag{15}$$

which must be solved for each energy on the complex contour and for each $\mathbf{k}$ point in the Brilouin zone or for an infinite cluster in real space. However, if the difference in potential function is small, i.e.,

$$\Delta\tilde{\mathbf{P}} = \tilde{\mathbf{P}}^{(i+1)} - \tilde{\mathbf{P}}^i \ll 1, \tag{16}$$

one need only solve (15) for a single-site cluster in real space. In this case charge self-consistency may be obtained on the basis of a CPA self-consistency loop formed by the approximate but much more efficient equations (5) and (15), which, including spd states, only involves matrices of size 9×9.

In most cases the condition (16) is satisfied simply because the mixing parameter x used to construct the input charge density for iteration $i + 1$

$$n_{\rm in}^{(i+1)} = xn_{\rm out}^i + (1 - x)n_{\rm in}^i \tag{17}$$

from the output $n_{\rm out}$ and input $n_{\rm in}$ charge densities of the current iteration i typically is of the order of a few percent, i.e., $x \ll 1$. Hence the difference in input charge density $\delta n = n_{\rm in}^{(i+1)} - n_{\rm in}^i \ll 1$ and as a rule the difference in the coherent potential function $\delta\tilde{P}$ will also be small. The only exception may occur when one of the potential functions has a pole in the energy range of interest because in that case even small changes in the electron density may lead to a large change in potential function difference. However, owing to the complex contour integration technique the effect will only be appreciable if the pole occurs close to the Fermi level and in that case it may be moved out of the energy range by a shift of representation. It follows that, by a judicious choice of mixing parameter x and LMTO representation α, the condition (16) may always be satisfied and thereby lead to an efficient two-step self-consistency procedure analogous to those used in standard LMTO bulk calculations and in the LMTO Green's-function technique.

III. THE SURFACE-LMTO-CPA METHOD

A. The surface Korringa-Kohn-Rostoker ASA Green's function

The system of coupled CPA equations (4) and (5) written for a disordered bulk crystal may be reformulated to treat the case of a surface of a disordered alloy, i.e.,

$$\tilde{g}_{\Lambda\Lambda}^\beta(z) = (A_{\rm SBZ})^{-1} \int_{\rm SBZ} d\mathbf{k}_\| \, \tilde{g}_{\Lambda\Lambda}^\beta(\mathbf{k}_\|, z), \tag{18}$$

$$\tilde{P}_\Lambda^\beta(z) = c_\Lambda P_\Lambda^{\beta A}(z) + (1 - c_\Lambda) P_\Lambda^{\beta B}(z)$$
$$+ [P_\Lambda^{\beta A}(z) - \tilde{P}_\Lambda^\beta(E)] \tilde{g}_{\Lambda\Lambda}^\beta(z)$$
$$\times [P_\Lambda^{\beta B}(z) - \tilde{P}_\Lambda^\beta(z)], \tag{19}$$

where Λ is a layer index, A_{SBZ} is the area of the two-dimensional (2D) Brilouin zone, c_Λ is the concentration of the alloy component A in the Λ layer, and β denotes the most localized, tight-binding LMTO representation,[12] which is used in the calculation of the surface Green's function.

The 2D Green's-function matrices $\tilde{g}_{\Lambda\Lambda}^\beta(\mathbf{k}_\parallel, z)$, which enter the integral (18), may be obtained in a number of ways. For instance, Kudrnovsky, Weinberger, and Drchal[8] applied a system of recurrent equations with appropriate boundary conditions to obtain a self-consistent surface Green's function. In the present work we prefer to use the technique implemented by Skriver and Rosengaard[4] based on the Dyson equation

$$\{1 + \tilde{g}^{\beta u}(\mathbf{k}_\parallel, z)[\tilde{\mathbf{P}}^\beta(z) - \tilde{\mathbf{P}}^{\beta u}(z)]\}\tilde{g}^\beta(\mathbf{k}_\parallel, z)$$

$$= \tilde{g}^{\beta u}(\mathbf{k}_\parallel, z), \tag{20}$$

which gives the coherent surface Green's-function matrix in terms of the Green's function $\tilde{g}^{\beta u}$ and potential function $\tilde{\mathbf{P}}^{\beta u}$ matrices of the unrelaxed semi-infinite crystal.

The complete procedure may be described as follows. First, we solve the bulk CPA problem including charge self-consistency. Then we construct the so-called ideal Green's function for the semi-infinite disordered crystal by means of the principal layer technique first implemented by Wenzien et al.[18] and recently applied in the calculation of stacking fault energies by Rosengaard and Skriver.[19] Next, we join this ideal Green's function and the analogous Green's function for a semi-infinite vacuum to form the unrelaxed surface Green's function $\tilde{g}^{\beta u}$. Finally, we iterate the system of CPA equations (18)–(20) and the charge self-consistency loop (6)–(8) to completion by means of the efficient two-step procedure described in Sec. II.

B. The Madelung potential and energy

The electrostatic part of the one-electron potential in the spheres may be written in the one-center form

$$V_C(\mathbf{r}) = \sum_{RL} V_{C;R}(r_R) Y_L(\hat{\mathbf{r}}_R), \tag{21}$$

i.e., as an atom-centered cubic-harmonic expansion. In the ASA we use only the spherically symmetric, i.e., $L = s$, part of the *potential*, and hence the potential in the atomic sphere at Λ in the two-dimensional unit cell is approximated by

$$V_{C;\Lambda}(r_\Lambda) = V_{C;\Lambda s}(r_\Lambda) Y_s + \frac{1}{S} \sum_{\Lambda' L'} M_{\Lambda\Lambda'}^{sL'} \bar{Q}_{\Lambda'}^{L'}. \tag{22}$$

Here the intrasphere contribution is obtained by numerical integration of the radial Poisson equation, M denotes the multipole (Madelung) matrices given in Ref. 4,

S is the atomic sphere radius, and $\bar{Q}$ is the average L-decomposed charge transfer for the alloy atoms at the layer Λ

$$\bar{Q}_\Lambda^L = c_\Lambda Q_\Lambda^{LA} + (1 - c_\Lambda) Q_\Lambda^{LB}, \tag{23}$$

$$Q_\Lambda^{Lj} = \frac{\sqrt{4\pi}}{2l+1} \int_{R_\Lambda} d\mathbf{r}\, Y_L(\hat{\mathbf{r}})^* \left(\frac{r}{S}\right)^l n_\Lambda^j(\mathbf{r}) - Z_\Lambda^j \delta_{l,s} \tag{24}$$

obtained from the total nonspherical charge density $n_\Lambda^j(\mathbf{r})$ inside the atomic sphere of A or B at the layer Λ. In the present implementation we include only $L = s, p$ in the multipole expansion and the dipole potential barrier has two contributions, one from the monopoles, i.e., the net charges in the spheres, and one from the dipole charges in the spheres. These contributions are of the same order of magnitude but have opposite signs, and it is only when they are combined in the self-consistency procedure that one obtains an accurate estimate of the dipole barrier.

The total energy of the disordered surface may be obtained from (11) and (12) if R is substituted by Λ and the Madelung energy

$$E_M = \frac{1}{2S} \sum_{\Lambda L, \Lambda' L'} \bar{Q}_\Lambda^L M_{\Lambda\Lambda'}^{LL'} \bar{Q}_{\Lambda'}^{L'} \tag{25}$$

calculated from the average mono- and dipole moments. For the three alloy systems considered here the moments Q_Λ^{LA} and Q_Λ^{LB} are found to be approximately equal to the average charge transfer over the the whole concentration range (see Table I, where the charge transfer for the components of alloys at the equiatomic concentration are presented as an example). Thus the Madelung energy (25) based on the approximation (23) may safely be used.

C. Integration technique

Since the off-diagonal elements of the Green's-function matrix may not in general be left invariant under the operations of the crystallographic point group, an efficient evaluation of the Brillouin-zone integrals, (4) and (18), requires the knowledge of the matrices $U(T)$ representing the transformations of the lattice harmonics Y under the point group operations T. In the bulk case the procedure is well known[6,20] and (4) may be rewritten as

$$\tilde{g}^\beta(z) = (V_{\text{BZ}})^{-1} \int_{\text{IBZ}} d\mathbf{k} \sum_T U(T) [\tilde{\mathbf{P}}^\beta(z) - \mathbf{S}^\beta(\mathbf{k})]^{-1}$$

$$\times U(T)^{-1}, \tag{26}$$

where the integration runs over the usual irreducible part of the Brillouin zone (IBZ). For cubic crystals, $l_{\max} \leq 2$, and in the basis of the cubic harmonic, as can easily be shown using the orthogonality relations, (26) may even be simplified further

I. A. ABRIKOSOV AND H. L. SKRIVER

$$\tilde{g}^{\beta}_{\lambda\lambda'}(z) = g^{\beta}_{\lambda\lambda'}(z)\delta_{\lambda\lambda'},$$

$$g^{\beta}_{\lambda\lambda}(z) = (V_{BZ})^{-1} \int_{IBZ} d\mathbf{k} \, \frac{1}{N_{\Gamma}} \sum_{\mu=1}^{N_{\Gamma}} g_{\lambda\mu,\lambda\mu}(\mathbf{k},z), \qquad (27)$$

$$g_{\lambda\mu,\lambda\mu}(\mathbf{k},z) = \{[\tilde{\mathbf{P}}^{\beta}(z) - \mathbf{S}^{\beta}(\mathbf{k})]^{-1}\}_{lm,lm}.$$

Here λ denotes the irreducible representation of the cubic group ($\Gamma^1, \Gamma^{15}, \Gamma^{12}$, and $\Gamma^{25'}$), N_{Γ} is the dimension of the corresponding representation, μ refers to the index within the representation, and l, m belong to the same representation as λ, μ.

The integration over the surface Brillouin zone (18) is less simple to perform because of the loss of symmetry. In this case we have to use the expression, analogous to (26) directly

$$\tilde{g}^{\beta}_{\Lambda\Lambda}(z) = (A_{SBZ})^{-1} \int_{ISBZ} d\mathbf{k}_{\parallel} \sum_T U(T) \, \tilde{g}^{\beta}_{\Lambda\Lambda}(\mathbf{k}_{\parallel},z)$$

$$\times U(T)^{-1}, \qquad (28)$$

where the integration runs over the irreducible part of the surface Brillouin zone (ISBZ) and the T summation runs over those symmetry elements which belong both to the surface and the bulk.

To perform the bulk Brillouin-zone integration (27) we have used the uniform k mesh,[16] which makes it possible to calculate the coherent Green's function (4) and solve the CPA equation (5) simultaneously, and which is therefore very fast and efficient.[13,15,16,21] The convergence of the scheme depends on the absolute number of k points rather than on their density, and we find that 500 k points in the irreducible part of the fcc Brillouin zone are usually sufficient to yield accurate *bulk* thermodynamic properties. Compared to any other CPA scheme, where a similar number of k points are used, the uniform k mesh[16] is much more efficient because it takes only one iteration to solve the CPA equations (4) and (5) self-consistently.

On the other hand, if we want to use the uniform k mesh in surface calculations, it would again be necessary to use approximately 500 k points, and the method would be much less efficient. Hence, in this case we have performed the integration (28) by means of the special points technique[22] using 36 k points in the irreducible part of the fcc 001 surface Brillouin zone. The maximal number of iteration for the system of equations (18)–(20) turned out to be 5, and to obtain comparable convergence of bulk and surface calculations the number k points in the evaluation of (27) was increased to 1500.

D. Details of calculation

The bulk calculations for the pure elements were performed by means of the tight-binding LMTO method within the nearly orthogonal representation[12] and all surface calculations were performed by means of the tight-binding LMTO Green's-function technique[4] in the most localized representation employing s, p, and d orbitals only. The complex integrals (8) were evaluated on a semicircular contour by means of 20 energy

points distributed so as to increase the sampling near the Fermi level. Exchange and correlation were included within the local-density approximation using the Perdew-Zunger parametrization[23] of the many-body calculations of Ceperley and Alder.[24] The surface region of the alloy treated self-consistently consisted of four layers of atom-filled spheres and two layers of vacuum spheres. Charge neutrality was maintained by placing the extra charge of the surface region in a fifth layer in the alloy region. The extra charge converged to approximately 0.0001 electrons and could safely be neglected in the calculation of the total energy.

IV. RESULTS AND DISCUSSION

In the following we shall present calculated equilibrium lattice spacings, mixing enthalpies, surface energies, and work functions for three fcc-based random alloys. In addition we present a segregation analysis for (100) surfaces of Cu-Ni, Ag-Pd, and Au-Pt based on the calculated surface energies obtained over the complete concentration range.

A. Bulk thermodynamic properties

The lattice parameters obtained by the bulk LMTO-CPA technique described in Sec. II and calculated as functions of alloy concentration are shown in Fig. 1. To bring out the concentration dependence and to facilitate the comparison with experimental values[25] we have in each case subtracted the calculated or experimental lattice spacing of the pure transition metal, i.e., Ni, Pd, or Pt. Therefore the deviation at 100% concentration is a measure of the error in the calculated lattice spacing of the pure metals.

From Fig. 1 it may be seen that the LMTO-CPA calculations give a correct description of the essentially linear concentration dependence found experimentally. Such a linear behavior is expected if the lattice mismatch between the alloy components and if the chemical shift as expressed by the charge transfer from the noble to the transition metal are small. Since both the lattice mismatch (see Fig. 1) and the charge transfer (see Table I) attain their largest values in the Ag-Pd system, it is quite satisfactory that the calculation predict a small negative deviation from the linear behavior in complete agreement with the experimental variation in this system.

The maximum deviation between the calculated and the measured lattice spacings is approximately 3%, which is the usual error in local-density calculations. Here one should note that the values for the pure metals are obtained by the LMTO method not including the effect of disorder. The fact that the disordered alloy calculations extrapolate exactly to the pure lattice spacing at either end of the concentration range means that the CPA does not introduce additional *methodical* errors.

In Fig. 2 we present the calculated mixing enthalpies for the three alloy systems under consideration and compare them with experimental data.[26,27] It may be seen that the LMTO-CPA calculations give a correct description of the concentration dependence found experimen-

tally. This includes the prediction of the asymmetry in the mixing enthalpy with respect to the equiatomic concentration. Thus the mixing enthalpy of the transition metals rich alloys are larger then those of the corresponding noble-metal-rich alloys.

The mixing enthalpy of disordered Ag-Pd alloys is found to be negative over the whole concentration range. This is a manifestation of the short-range order which is known to exist in Ag-Pd alloys[28] and which makes the alloy components tend to surrounded themselves with unlike atoms. The single-site CPA correspond to a completely disordered alloy and does not include the effect of short-range order. It is therefore to be expected that the calculated mixing enthalpy of Ag-Pd alloys is higher

TABLE II.   Impurities solution energies in Cu-Ni system.

Impurity	Impurity solution energy, (eV)		
	Calc. values		Exp.[b]
	This work	KKR-GF[a]	
Ni in Cu	-0.06	-0.08	0.04
Cu in Ni	0.07	0.20	0.12

[a] Reference 30.
[b] Recalculated from the mixing enthalpies of Ref. 26.

than experimental values determined from real alloys with short-range order. If one includes the effect of short-range order the agreement between theory and experiment may be improved considerably.[29]

The calculated mixing enthalpy in the Au-Pt system is positive, in complete agreement with the existence of a miscibility gap in the phase diagram of these alloys. This also means that the alloy components tend to be surrounded by atoms of their own kind. In this case the experimental mixing enthalpies[27] have been derived by an analysis of the miscibility gap under the assumption of complete disorder. It is therefore perhaps not surprising that the experimentally derived values are somewhat higher than the values obtained by the LMTO-CPA calculations.
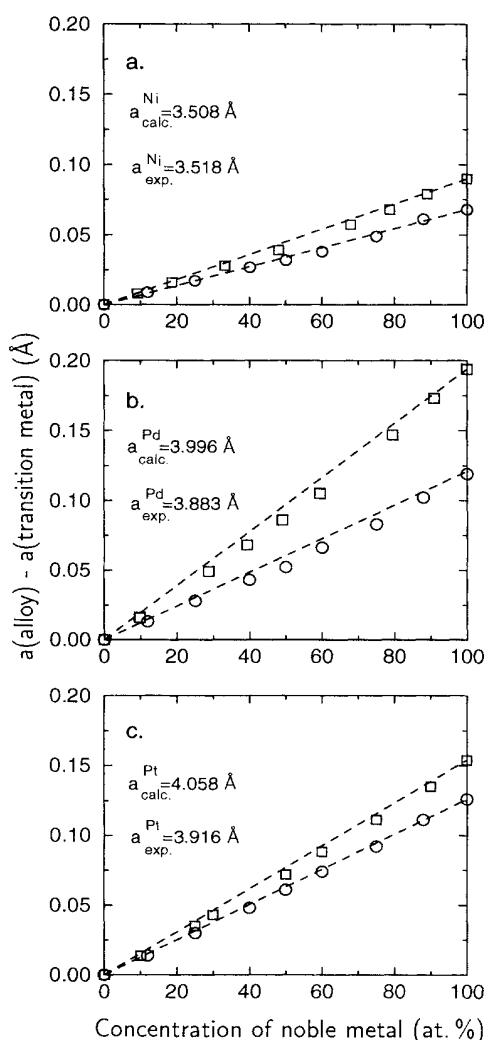

FIG. 1.   The lattice parameters for the (a) Cu-Ni, (b) Ag-Pd, and (c) Au-Pt alloys as functions of the noble-metal concentration. Calculated results are denoted by circles and experimental values by squares. The dashed lines represent the concentration average of the lattice parameters of the alloy components. To aid the comparison between theory and experiment the lattice constants of the pure transition metals have been subtracted from the alloy values.
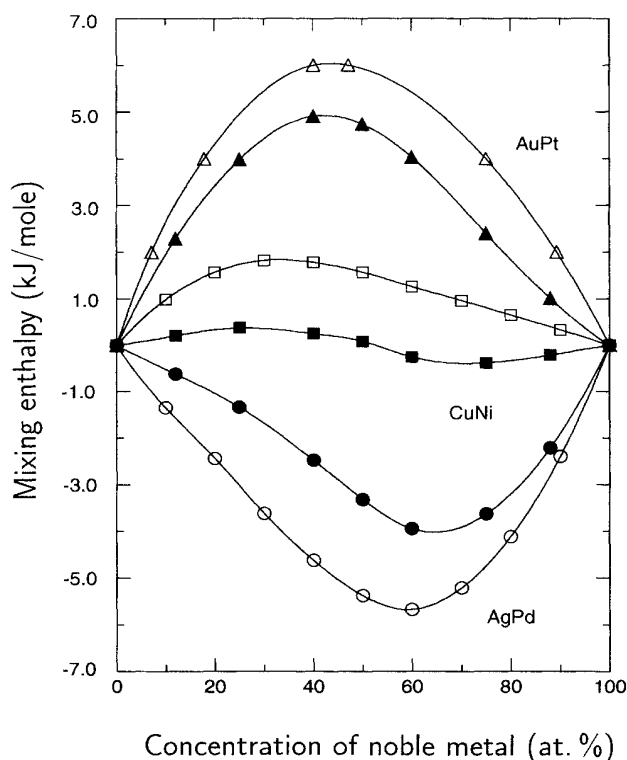

FIG. 2.   Mixing enthalpies for the Cu-Ni (squares), Ag-Pd (circles), and Au-Pt (triangles) alloys as a function of noble-metal concentration. Full symbols denote the calculated results of this work; open symbols denote the experimental data of Refs. 26 and 27.

The mixing enthalpy of the Cu-Ni system is the smallest of those calculated and is found to change sign as a function of concentration. This sign change is in disagreement with experiment,[26] but agrees with the impurity solution energies calculated for this system by the Korringa-Kohn-Rostoker (KKR) Green's-function technique,[30] as may be seen in Table II. The mixing enthalpy for the Cu-Ni system obtained by the Connoly-Williams method[31] and the embedded-atom method[32] is positive over the whole concentration range in agreement with experiment. On the other hand, both calculations[31,32] overestimate the mixing enthalpy in both the Ag-Pd and the Au-Pt system to the extent that the enthalpy in Ag-Pd obtained in Ref. 32 is completely positive, in disagreement with the experimental data and the Ag-Pd phase diagram. One may therefore speculate that a similar overestimate in the Cu-Ni system is the cause of the seemingly good agreement between experiment and the Connoly-Williams and embedded-atom-method results.

B. Unsegregated surface properties

In Fig. 3 we present the surface energy of fcc 001 surfaces of random Cu-Ni, Ag-Pd, and Au-Pt alloys as obtained by the LMTO-CPA surface technique described in Sec. III. The calculations were performed at the theoretical lattice parameters presented in Sec. IV A neglecting lattice relaxation and surface segregation, i.e., the atomic positions and the alloy concentrations were kept unchanged at their bulk values up to and including the surface layer.

It may be seen from Fig. 3 that the calculated surface energies vary almost linearly with concentration between the values obtained for the pure elements. The deviation from the linear behavior may be used as a measure of the effects of alloying, and judged from the figure these effects are generally small. The largest effect is found in the Cu-Ni system and in Fig. 4 we have therefore compared the calculated deviation from the linear behavior for this

FIG. 4. The calculated (full squares) deviations from the linear behavior of the surface energy ($\Delta E_{surf} = E_{surf}^{alloy} - c_{bulk}^{Cu} E_{surf}^{Cu} - c_{bulk}^{Ni} E_{surf}^{Ni}$) as a function of Cu concentration in the Cu-Ni system, compared to the experimental one (open squares) (Ref. 34).

system with the results of measurements of the surface tension of the liquid alloys.[33,34]

In the comparison with experiment, Fig. 4, one should note that the measured surface tension includes an entropy term proportional to the melting temperature which is commonly subtracted to obtain a surface energy.[35] In order to avoid this procedure we show the deviation from the linear behavior instead of the surface energy itself, expecting the entropy contribution to the deviation to be negligible. Furthermore, the calculated surface energy corresponds to the unsegregated alloy while the measured surface tension includes the effect of segregation even at the elevated temperatures.[34] According to recent model tight-binding CPA calculations[36] one expects the unsegregated alloy to show a positive deviation from the linear behavior while the segregated alloy exhibits a negative deviation, in qualitative agreement with the results in Fig. 4. Hence it appears that
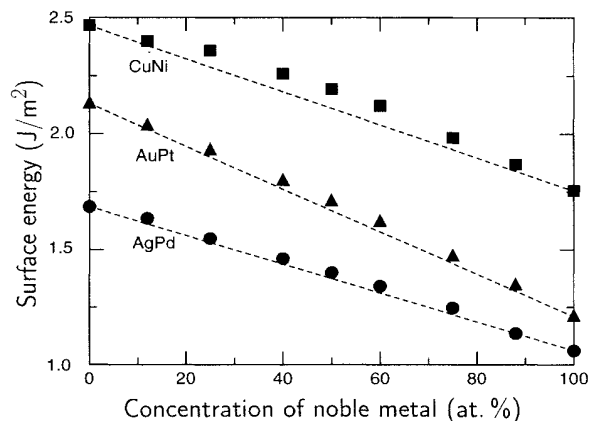

FIG. 3. Calculated surface energy concentration dependences for the (001) surfaces of Cu-Ni (squares), Ag-Pd (circles), and Au-Pt (triangles) alloys.
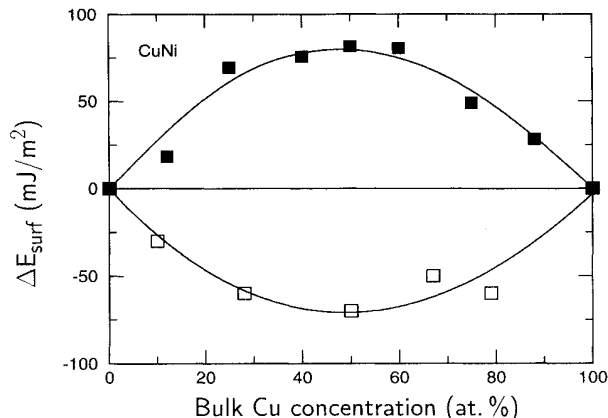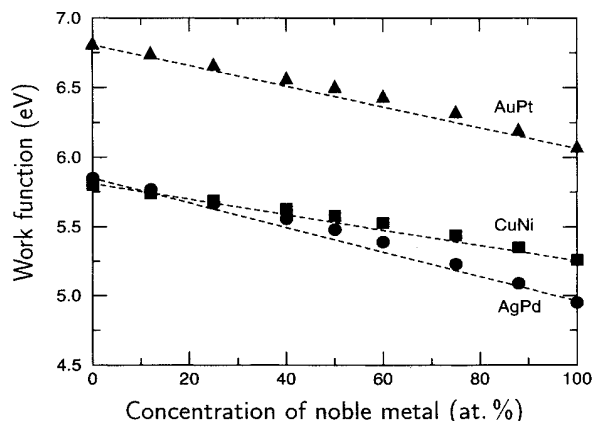

FIG. 5. Calculated work-function concentration dependences for the (001) surfaces of Cu-Ni (squares), Ag-Pd (circles), and Au-Pt (triangles) alloys.
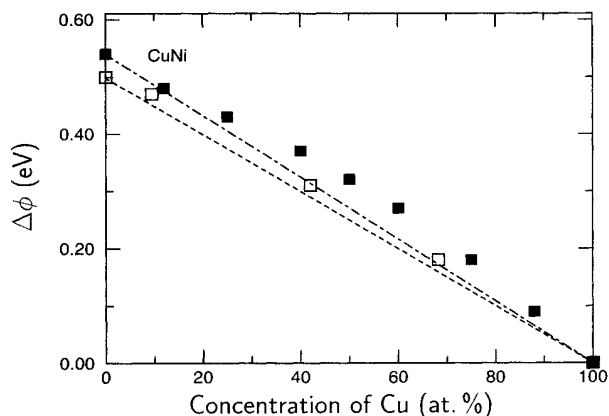
FIG. 6. Comparison between the calculated (full squares) and the experimental (open squares) (Ref. 37) concentration dependences of the work function $\Delta\phi = \phi_{\text{alloy}} - \phi_{\text{Cu}}$ for Cu-Ni system ($\phi_{\text{Cu}}^{\text{theory}} = 5.3$ eV, $\phi_{\text{Cu}}^{\text{exp}} = 4.6$ eV). The concentration average of the pure Cu and pure Ni work functions are denoted by the dot-dashed line (theory) and dashed line (experiment).

$$F_\Lambda(c_\Lambda) = E_\Lambda(c_\Lambda) - TS^{\text{conf}}(c_\Lambda), \qquad (29)$$

where c_Λ is the layer-dependent noble-metal concentration. Thus the influence of the vibrational entropy on the segregation is negelcted.

(2) The internal energy per atom in layer Λ depends on the concentration in this layer only. Hence the internal energy per atom at the surface of concentration c_s of an alloy may be taken to be the internal energy per atom at the surface of the *unsegregated* alloy with bulk concentration c_b equal to c_s.

(3) Both the surface and the bulk alloy are completely disordered so that the configurational entropy term is

the LMTO-CPA calculations give a correct description of the concentration dependence of the surface energies of the unsegregated Cu-Ni, Ag-Pd, and Au-Pt alloys which may be used as the basis for a surface segregation analysis within an appropriate thermodynamic model.

In Fig. 5 we present the calculated work functions of fcc 001 surfaces of random Cu-Ni, Ag-Pd, and Au-Pt alloys. Again we observe an almost linear variation with concentration indicating that the effect of alloying is small. The calculated change in the work function with concentration for the Cu-Ni system is shown in Fig. 6 together with experimental results.[37] In this case the measured work function is plotted as a function of the surface concentration and may therefore be compared directly with the unsegregated values of the corresponding bulk concentration. It appears that the change in the work function with concentration is correctly reproduced by the calculations.

C. Surface segregation analysis

The surface segregation in alloys of group VIIIB transitions metals with the noble metals has been studied experimentally[38-43] by Monte-Carlo simulations,[44,45] as well as theoretically by a semiempirical scheme,[28,46] by a tight-binding Hartree Hamiltonian,[47] or by means of a model alloy state density.[48] In the present study we shall use our *ab initio* layer decomposed surface energies in conjunction with the thermodynamic model of Brejnak and Modrak[48] to determine the noble-metal concentration in the surface layer of a disordered alloy.

The basic assumptions of the thermodynamic model are as follows.[48]

(1) The free energy F_Λ of the Λth layer of the alloy is the sum of the internal energy E_Λ per atom in this layer and the configurational entropy term S^{conf}
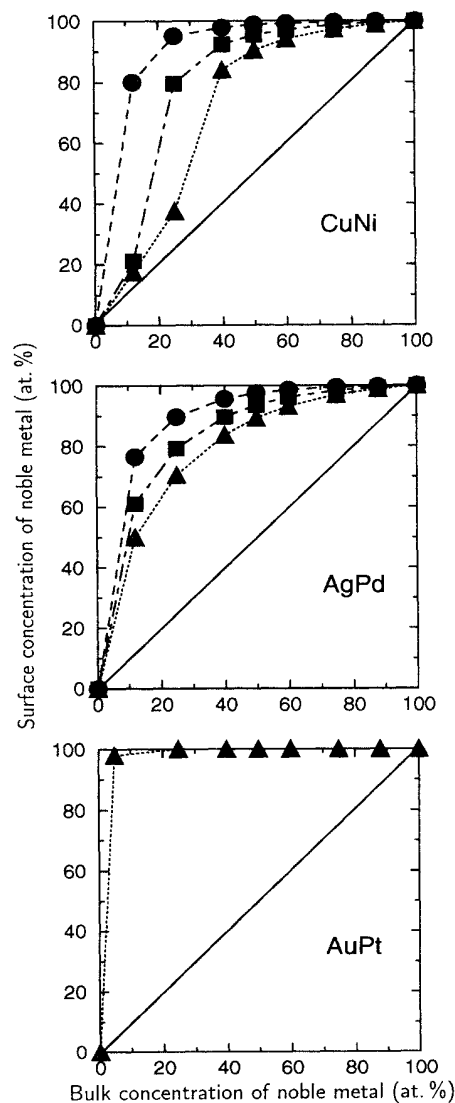

FIG. 7. Calculated concentrations of the noble metals at the (001) surfaces of Cu-Ni, Ag-Pd, and Au-Pt alloys as a function of bulk noble-metal concentration. The results for the different temperatures (500 K, circles; 700 K, squares; and 900 K, triangles) are presented. Full lines indicate the case of the unsegregated alloys.

given by the expression

$$S^{\text{conf}}(c_\Lambda) = -k_B[c_\Lambda \ln(c_\Lambda) + (1 - c_\Lambda) \ln(1 - c_\Lambda)], \quad (30)$$

which neglects short-range-order effects.

(4) The only layer affected by the presence of the surface is the surface layer itself, which mean that we are not able to obtain a surface concentration profile.

With these assumptions the equation governing the surface concentration has the form[48]

$$\left.\frac{\partial E_b(c)}{\partial c}\right|_{c=c_b} - \left.\frac{\partial E_s(c)}{\partial c}\right|_{c=c_s} + k_B T \ln\left[\frac{c_b(1 - c_b)}{c_s(1 - c_s)}\right] = 0,$$

$$(31)$$

where indices b and s refer to an atom in the bulk or at the surface, respectively. To solve (31) we have approximated the calculated concentration dependences of the internal energies E_b and E_s by second-order polynomials obtained by least-squares fit.

The noble-metal concentration at the surface layer in disordered Ni-Cu, Ag-Pd, and Au-Pt alloys obtained by (31) as a function of the noble-metal concentration in the bulk is presented in Fig. 7. It may be seen that the noble metals in all cases exhibit a strong tendency to segregate and that the surface excess decreases with increasing temperature due to the entropy term. The segregation is governed by the differences in the surface energies of the pure constituents because by migrating to the surface the noble metals will lower the surface energy of the alloy. As a result, the strongest segregation is found in the Au-Pt system where the surface energy difference between the constituents is the largest within the three systems treated, and this means that gold will cover the surface of its alloys even at low concentration and at high temperatures. Our results for the surface segregation agree with both experimental data[38-43] and with Monte Carlo simulations.[44,45]

V. SUMMARY

This paper reports the implementation of a self-consistent coherent-potential technique for calculating ground-state properties of random substitutional alloys and their surfaces. The ground state is found within the local-density approximation, and the coherent-potential technique is based on the linear-muffin-tin-orbitals method in the atomic sphere approximation and the tight-binding representation.

The method is applied in *ab initio* calculations of bulk and surface properties of three fcc-based alloys Cu-Ni, Ag-Pd, and Au-Pt. The calculated concentration dependence of the lattice parameters agree with experiment with a maximum deviation between theory and experiment of 3%. The theoretical mixing enthalpies for the Ag-Pd and the Au-Pt alloys are negative and positive, respectively, and agree with experimental data over the whole concentration range. In the Cu-Ni system the calculated mixing enthalpy changes sign as a function of concentration being slightly negative at high Cu concentrations. This is in contrast to the experimentally derived enthalpy which is positive for all concentrations but agrees with recent KKR Green's-function calculations.

The calculated work functions and surface energies for the 001 surface of the random alloys exhibit an almost-linear variation with concentration. In the Cu-Ni system the work function is found to have a positive deviation from the linear behavior in agreement with experiment. It is furthermore shown that the calculated surface energy may agree with experiment if the effect of surface segregation is taken into account.

The concentration of the noble metals at the fcc 001 surface of Cu-Ni, Ag-Pd, and Au-Pt alloys is calculated from the unsegregated surface energies within a simple thermodynamic model. It is found that the noble metals segregate towards the surfaces of their alloys for all bulk concentration. The segregation is found to be particularly strong in the Au-Pt system and this means that Au will completely cover the surface of its alloys.

ACKNOWLEDGMENTS

[1] W. Lambrecht and O. K. Andersen, Surf. Sci. **178**, 256 (1986); and (private communication).

[2] J. E. Inglesfield and G. A. Benesh, Phys. Rev. B **37**, 6682 (1988).

[3] J. M. MacLaren, S. Crampin, D. D. Vvedensky, and J. Pendry, Phys. Rev. B **40**, 12 164 (1989).

[4] H. L. Skriver and N. M. Rosengaard, Phys. Rev. B **43**, 9538 (1991).

[5] H. L. Skriver and N. M. Rosengaard, Phys. Rev. B **46**, 7157 (1992).

[6] A. Gonis, *Green Function for Ordered and Disordered Systems* (North-Holland, Amsterdam, 1992).

[7] D. D. Johonson, D. M. Nicholson, F. J. Pinsky, B. L. Gyorffy, and G. M. Stocks, Phys. Rev. B **41**, 9701 (1990).

[8] J. Kudrnovsky, P. Weinberger, and V. Drchal, Phys. Rev. B **44**, 6410 (1991).

[9] J. Kudrnovsky, I. Turek, V. Drchal, P. Weinberger, N. E. Christensen, and S. K. Bose, Phys. Rev. B **46**, 4222 (1992).

[10] J. M. MacLaren, A. Gonis, and G. Schadler, Phys. Rev. B **45**, 14 392 (1992).

[11] O Gunnarsson, O. Jepsen, and O. K. Andersen, Phys. Rev. B **27**, 7144 (1983).

[12] O. K. Andersen, O. Jepsen, and D. Glötzel, in *Highlights of Condensed-Matter Theory*, edited by F. Bassani, F. Fumi, and M. P. Tosi (North-Holland, New York, 1985).

[13] I. A. Abrikosov, Yu. H. Vekilov, and A. V. Ruban, Phys. Lett. A **154**, 407 (1991).

[14] Z. W. Lu, S.-H. Wei, A. Zunger, S. Frota-Pessoa, and L. G. Ferreira, Phys. Rev. B **44**, 512 (1991).

[15] I. A. Abrikosov, Yu. H. Vekilov, P. A. Korzhavyi, A. V. Ruban, and L. Shilkrot, Solid State Commun. **83**, 867 (1992); A. V. Ruban and P. A. Korzhavyi (private com-

munication).

[16]H. Akai, J. Phys. Condens. Matter. **1**, 8045 (1989).

[17]H. L. Skriver, *The LMTO Method* (Springer, Berlin, 1984).

[18]B. Wenzien, J. Kudrnovský, V. Drchal, and M. Šob, J. Phys. Condens. Matter **1**, 9893 (1989).

[19]N. M. Rosengaard and H. L. Skriver, Phys. Rev. B (to be published).

[20]J. Molenaar, P. T. Coleridge, and A. Lodder J. Phys. C **15**, 6955 (1982).

[21]H. Ebert, B. Drittler, and H. Akai, J. Magn. Magn. Mat. **104-107**, 733 (1992).

[22]S. L. Cunningham, Phys. Rev. B **10**, 4988 (1974).

[23]J. Perdew and A. Zunger, Phys. Rev. B **23**, 5048 (1981).

[24]D. M. Ceperley and B. J. Alder, Phys. Rev. Lett. **45**, 566 (1980).

[25]W. B. Pearson, *A Handbook of Lattice Spacing and Structure of Metals and Alloys* (Pergamon, London, 1967).

[26]R. Hultgren, P. D. Desai, D. T. Hawkins, M. Gleiser, and K. K. Kelley, *Selected Values of Thermodynamic Properties of Binary Alloys* (American Society for Metals, Metals Park, OH, 1973).

[27]H.-J. Schaller, Z. Metallkde. **70**, 354 (1979).

[28]V. Kumar, D. Kumar, and S. K. Joshi, Phys. Rev. B **19**, 1954 (1979).

[29]I. A. Abrikosov, Y. H. Vekilov, A. V. Ruban, and D. Ya. Kats, Solid State Commun. **80**, 177 (1991).

[30]B. Drittler, M. Weinert, R. Zeller, and P. H. Dederichs, Phys. Rev. B **39**, 930 (1989).

[31]S. Takizawa, K. Terakura, and T. Mohri, Phys. Rev. B **39**, 5792 (1989).

[32]R. A. Johnson, Phys. Rev. B **41**, 9717 (1990).

[33]V. V. Fesenko V. N. Eremenko, and M. I. Vasiliu, Zh. Fiz. Khim. **35**, 1750 (1961).

[34]J. G. Eberhart, J. Phys. Chem. **70**, 1183 (1966).

[35]F. R. de Boer, R. Boom, W. C. M. Mattens, A. R. Miedema, and A. K. Niessen, *Cohesion in Metals* (North-Holland, Amsterdam, 1988).

[36]I. Ishida, J. Phys. Soc. Jpn. **56**, 1427 (1987).

[37]Y. Takasu, H. Konno, and T. Yamashina, Surf. Sci. **45**, 321 (1974).

[38]*Interfacial Segregation*, edited by W. C. Johnson and J. M. Blakely (American Society for Metals, Metals Park, OH, 1979).

[39]K. Watanabe, M. Hashiba, and T. Yamashina, Surf. Sci. **61**, 483 (1976).

[40]G. P. Schwartz, Surf. Sci. **76**, 113 (1978).

[41]T. T. Tsong, Y. S. Ng, and S. B. McLane, J. Chem. Phys. **73**, 1464 (1980).

[42]T. S. King and R. G. Donnelly, Surf. Sci. **141**, 417 (1984).

[43]S. E. Hornström, L. I. Johansson, and A. Flodström, Appl. Surf. Sci. **26**, 27 (1986).

[44]H. Y. Wang, R. Najafabadi, D. J. Srolovitz, and R. LeSar, Phys. Rev. B **45**, 12 028 (1992).

[45]G. H. Vurens, F. C. M. J. M. Van Delft, and B. E. Nieuwenhuys, Surf. Sci. **192**, 438 (1987).

[46]V. Kumar, Phys. Rev. B **23**, 3756 (1981).

[47]S. Mukherjee, J. L. Moran-Lopez, V. Kumar, and K. H. Bennermann, Phys. Rev. B **25**, 730 (1982).

[48]M. Brejnak and P. Modrak, J. Phys. Condens. Matter. **2**, 869 (1990); Surf. Sci. **247**, 215 (1991).